ISSN 1063-7834, Physics of the Solid State, 2008, Vol. 50, No. 11, pp. 2088–2094. © Pleiades Publishing, Ltd., 2008.
Original Russian Text © I.S. Edelman, O.V. Vorotynova, V.A. Seredkin, V.N. Zabluda, R.D. Ivantsov, Yu.I. Gatiyatova, V.F. Valeev, R.I. Khaĭbullin, A.L. Stepanov, 2008, published in Fizika Tverdogo Tela, 2008, Vol. 50, No. 11, pp. 2002–2008.

MAGNETISM AND FERROELECTRICITY

Magnetic and Magneto-Optical Properties of Ion-Synthesized Cobalt Nanoparticles in Silicon Oxide

I. S. Edelman[a], O. V. Vorotynova[b], V. A. Seredkin[a], V. N. Zabluda[a], R. D. Ivantsov[a], Yu. I. Gatiyatova[c], V. F. Valeev[c], R. I. Khaĭbullin[c], and A. L. Stepanov[c, d]

[a] *Kirensky Institute of Physics, Siberian Branch, Russian Academy of Sciences, Akademgorodok, Krasnoyarsk, 660036 Russia*
e-mail: ise@iph.krasn.ru

[b] *Institute of Urban Construction, Management, and Regional Economics, Siberian Federal University, Svobodnyi pr. 79, Krasnoyarsk, 660041 Russia*

[c] *Zavoisky Physical-Technical Institute, Russian Academy of Sciences, Sibirskiĭ trakt 10/7, Kazan, 420029 Russia*

[d] *Laser Zentrum Hannover, Hollerithallee 8, Hannover, D-30419 Germany*

Received January 28, 2008

Abstract—The magnetic and magneto-optical properties of ion-synthesized cobalt nanoparticles in the amorphous silicon oxide matrix are investigated as a function of the implantation dose. The analysis of the field dependences of the magnetization and the magneto-optical Faraday and Kerr effects demonstrates that, as the ion implantation dose increases, the superparamagnetic behavior of an ensemble of cobalt nanoparticles at room temperature gives way to a ferromagnetic response with the anisotropy characteristic of a thin magnetic film. The magnetization curves for the superparamagnetic and ferromagnetic ensembles of cobalt nanoparticles are simulated to determine their average sizes and the filling density in the irradiated layer of the silicon dioxide matrix. It is revealed that the spectral dependences of the Faraday and Kerr effects for ion-synthesized cobalt nanoparticles differ substantially from those for continuous cobalt films due to the localized excitations of free electrons in the nanoparticles.

PACS numbers: 75.60.Ej, 78.20.Ls, 61.46.Df

DOI: 10.1134/S1063783408110140

1. INTRODUCTION

The demands for fast optical devices capable of recording, processing, and transmitting information have stimulated search for materials with improved magneto-optical parameters [1, 2]. One of the promising ways in this direction is the design of composite materials based on transition metal nanoparticles embedded in dielectric or semiconductors matrices. Specific features of the excitation of conduction electrons in metal nanoparticles in the visible range lead to a change in the spectral dependences of the off-diagonal components of the optical conductivity tensor responsible for the magneto-optical effects and can enhance these effects in necessary spectral ranges [3, 4].

The magnetic properties of nanocomposites prepared by implantation of cobalt ions into a TiO_2 single-crystal substrate are described in [5]. The magnetic anisotropy observed in these samples was explained by the influence of the crystallographic anisotropy of the TiO_2 matrix containing cobalt. In this respect, investigations into the magnetic properties of cobalt nanoparticles prepared by implantation into an amorphous matrix under ion irradiation conditions similar to those used in [5] are of special interest. For this purpose, in our work, a substrate consisting of silica glass, i.e., amorphous silicon dioxide (SiO_2), was chosen as a matrix. It is important to trace the evolution of the magneto-optical spectra of implanted samples by varying the implantation dose and to reveal the optimum conditions for the formation of samples that provide pronounced magnetic properties of an ensemble of nanoparticles, on the one hand, and the retention of a high transparency of the nanocomposite material, on the other hand.

This paper reports on the first results of investigations into the magneto-optical Faraday effect, as well as the magneto-optical polar and meridional Kerr effects, in an ensemble of cobalt nanoparticles produced in the amorphous silicon dioxide matrix with the use of the implantation technique as a function of the ion implantation dose. The results obtained are compared with the data of investigations into the magneto-optical effects in Co/SiO_2 granular multilayer films prepared by ion-plasma deposition.

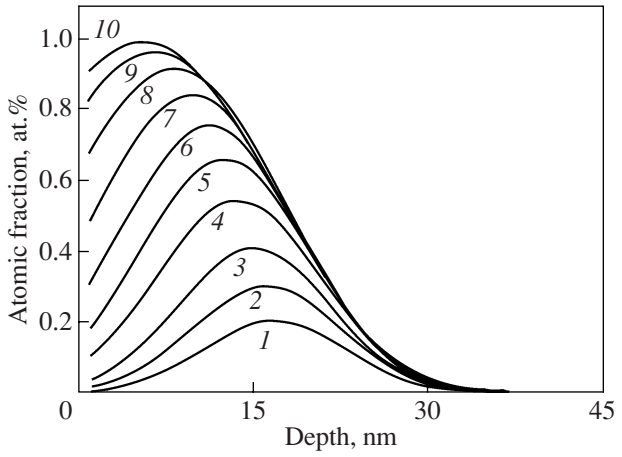

Fig. 1. Calculated concentration distribution profiles of implanted cobalt impurities over the depth in the silicon dioxide (SiO_2) matrix upon implantation of cobalt ions with an energy of 40 keV at the ion doses D = (*1*) 0.6, (*2*) 0.9, (*3*) 1.1, (*4*) 1.6, (*5*) 1.9, (*6*) 2.3, (*7*) 2.8, (*8*) 3.3, (*9*) 3.8, and (*10*) 4.3×10^{15} ions/cm^2.

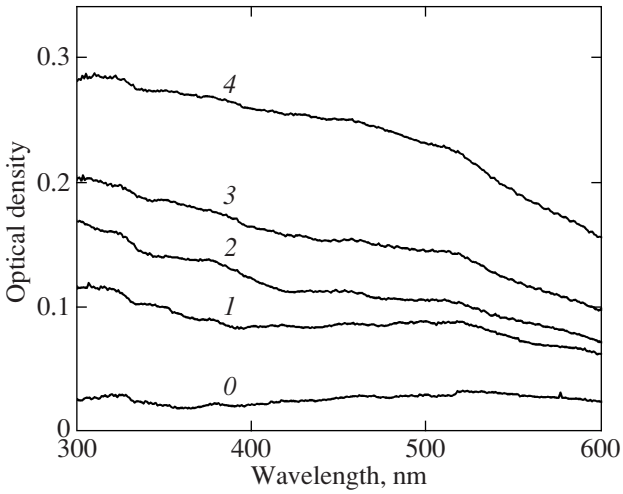

Fig. 2. Optical density spectra of the composite samples formed at the ion doses D = (*1*) 0.25, (*2*) 0.50, (*3*) 0.75, and (*4*) 1.00×10^{17} ions/cm^2. Curve *0* indicates the spectrum of the unimplanted glass.

2. SAMPLE PREPARATION AND EXPERIMENTAL TECHNIQUE

2.1. Sample Preparation

Cobalt nanoparticles were formed in the SiO_2 matrix by implantation of low-energy Co^+ ions (40 keV) at different doses $D = 0.25 \times 10^{17}$ (sample **1**), 0.50×10^{17} (sample **2**), 0.75×10^{17} (sample **3**), and 1.00×10^{17} (sample **4**) ions/cm^2. The implantation was performed at room temperature on an ILU-3 ion beam accelerator at a residual pressure of the order of 10^{-5} Torr [6]. The current density of the ion beam was maintained approximately equal to 8 μA/cm^2 in order to prevent uncontrollable heating of the glass target.

The distribution profile of implanted cobalt ions in the glass was simulated with the computer program (DYNA algorithm) [7] based on consideration of pair collisions of implanted ions with substrate atoms, which leads to a change in the phase state of the surface layer of the target with due regard for its surface sputtering. Figure 1 shows the depth distributions of implanted ions at different implantation doses. In order to evaluate the distribution of implanted impurities in the sample before the formation of metal nanoparticles, the calculations were performed with doses somewhat lower than those used in experiments.

It can be seen from Fig. 1 that the thickness of the implanted layer in the samples is of the order of 30 nm and the peak of the concentration of implanted cobalt impurities increases and shifts toward the surface with an increase in the implantation dose. As a result, the metal concentration in the vicinity of the surface at higher doses can reach considerable values, which exceed the metal solubility in the glass. This leads to the formation of cobalt nanoparticles in the implanted layer of the substrate. The formation of cobalt nanoparticles upon cobalt implantation into SiO_2 substrates at high doses was previously revealed in [8–10]. Spherical cobalt nanoparticles were observed in cross sections of implanted samples with the use of transmission electron microscopy, and their sizes were approximately equal to 3–8 nm at an ion dose of 1.0×10^{17} ions/cm^2.

The optical absorption (optical density) spectra of composite materials were recorded in the range 300–600 nm (Fig. 2). As can be seen from Fig. 2, the absorption of the sample increases with an increase in the irradiation dose due to the increase in the number of radiation-induced defects in the glass, as well as owing to the formation of cobalt nanoparticles and the increase in their concentration in the implanted layer. As is known, the radiation-induced defects are responsible for the optical absorption in the irradiated SiO_2 oxide in the near-UV spectral range at wavelengths shorter than ~350 nm [11]. Therefore, the magneto-optical measurements were carried out at wavelengths larger than 350 nm at which the absorption by cobalt nanoparticles is dominant.

2.2. Technique of Magnetic and Magneto-Optical Measurements

The magnetic properties of the synthesized composite materials were investigated using induction magnetometry. The dependences of the induced magnetic moment on the magnetic field applied either parallel to the plane (in-plane geometry) or perpendicular to the plane (out-of-plane geometry) of the sample were measured at room temperature on a magnetometer with a magnetic field sweep of up to 500 mT. When processing the data of the magnetic measurements, the diamagnetic contribution of the substrate was subtracted and

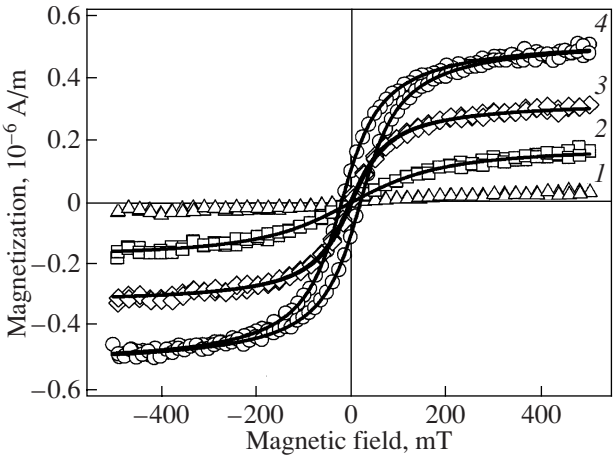

Fig. 3. Experimental magnetization curves measured in the plane of the samples at room temperature for the composite materials based on the SiO_2 plates with cobalt nanoparticles formed at the ion doses D = (*1*) 0.25, (*2*) 0.50, (*3*) 0.75, and (*4*) 1.00×10^{17} ions/cm^2. Solid lines represent the results of the simulation of the experimental curves according to relationships (1) and (2).

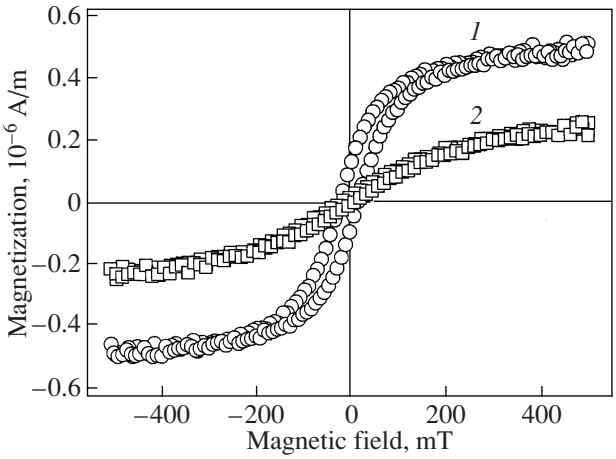

Fig. 4. Experimental magnetization curves for the composite material based on the SiO_2 plate with cobalt nanoparticles formed upon implantation at an ion dose of 1.0×10^{17} ions/cm^2 for two limiting orientations of the magnetic field, i.e., (*1*) in the plane of the plate and (*2*) perpendicular to the plane of the plate. T = 300 K.

the measured magnetic moment was reduced to the volume of the implanted layer in the sample in order to compare the magnetizations of the nanocomposite materials synthesized at different implantation doses.

The magneto-optical effects were measured using the azimuth modulation of the orientation of the plane of polarization of the light wave. The magneto-optical Faraday rotation was measured in the normal (out-of-plane) geometry as a function of the wavelength of the electromagnetic wave in the spectral range 500–1000 nm in external magnetic fields varying from –500 to +500 mT. The polar Kerr effect was measured in the spectral range 400–800 nm in magnetic fields of up to 1.4 T aligned parallel to the normal to the sample surface. The meridional Kerr effect for the *p* polarization of the light wave was measured at a wavelength of 550 nm in magnetic fields of up to 120 mT aligned parallel to the sample surface and the plane of incidence of light. The magneto-optical effects were measured accurate to within ±0.2 min.

3. RESULTS AND DISCUSSION

3.1. Magnetization Curves

Figure 3 depicts the magnetization curves obtained during the magnetic field scanning in the plane of the sample for the glasses with cobalt nanoparticles formed at different implantation doses D. At the small dose $D = 0.25 \times 10^{17}$ ions/cm^2, the composite samples at room temperature exhibit a paramagnetic response (Fig. 3, curve *1*). With an increase in the amount of implanted cobalt impurities to $D = (0.50–0.75) \times 10^{17}$ ions/cm^2, the irradiated glasses possess superparamagnetic properties (Fig. 3, curves *2*, *3*). At the maximum implantation dose $D = 1.0 \times 10^{17}$ ions/cm^2, the composite sample is characterized by a ferromagnetic response. This can be judged from the magnetic hysteresis loop with the following parameters: the coercive field is B_C = 18.5 mT, and the ratio between the remanent magnetization M_{rem} and the saturation magnetization M_{sat} is $M_{rem}/M_{sat} \sim 0.2$ (Fig. 3, curve *4*). Therefore, the dynamics of a change in the magnetic response of the silica glass with an increase in the concentration of implanted cobalt (nanoparticles) can be represented as the sequential transitions paramagnet–superparamagnet–ferromagnet at room temperature.

Investigations of the angular dependence of the magnetic hysteresis loop for the SiO_2 substrate irradiated at the maximum dose $D = 1.0 \times 10^{17}$ ions/cm^2 have revealed that the ferromagnetism of the composite material is characterized by an anisotropy of the easy-plane type, which is typical of thin ferromagnetic films. The magnetization curves measured for two limiting orientations of the magnetic field with respect to the plane of the composite material are shown in Fig. 4. The shape and the parameters of the hysteresis loop remain unchanged with a change in the orientation of the magnetic field in the in-plane geometry, which indicates that the magnetic anisotropy in the plane of the sample is absent. However, the magnetization upon scanning of the magnetic field applied perpendicular to the plane of the plate (out-of-plane geometry) does not reach saturation even at a maximum field of 500 mT (Fig. 4). Therefore, the inference can be made that the direction of the normal to the plane of the implanted plate is a hard magnetization axis.

As is known, the magnetic response of a nanocomposite (superparamagnetic or ferromagnetic) is very

sensitive to the size and a number of inclusions (nanoparticles) of the magnetic phase. In this respect, the average sizes of synthesized cobalt nanoparticles and the density of filling of the implanted layer with nanoparticles were estimated by simulating the experimental magnetization curves for the samples under investigation. The field dependence of the magnetization of the composite materials in the superparamagnetic state was simulated by the Langevin function [12]; that is,

$$M = M_S\left(\coth(x) - \frac{1}{x}\right), \quad (1)$$

where $x = M_{Co}\langle V\rangle B/kT$ is the dimensionless quantity, $M_S = NM_{Co}\langle V\rangle$ is the saturation magnetization of the nanocomposite system, $T = 300$ K is the temperature of measurements, and $M_{Co} = 1.435 \times 10^6$ A/m is the saturation magnetization of the hexagonal close-packed phase of metallic cobalt [12]. The average volume $\langle V\rangle$ and the concentration N of cobalt nanoparticles in the implanted layer in the Langevin formula were chosen as parameters varied in the course of the simulation. The results of the simulation for the superparamagnetic samples of the composite materials formed at of doses 0.50 and 0.75×10^{17} ions/cm^2 are presented in Fig. 3. It can be seen from this figure that model curves *2* and *3* constructed using formula (1) are in good agreement with the experimentally measured dependences of the magnetization of the synthesized materials on the applied field.

For the ferromagnetic sample prepared at the maximum implantation dose with a pronounced magnetic hysteresis loop, the field dependences of the magnetization were simulated using the formula proposed by Geiler et al. [13]; that is,

$$M = \frac{2NM_{Co}\langle V\rangle}{\pi}\arctan\left(\frac{B \pm B_C}{B_T}\right), \quad (2)$$

where M_{Co} is the saturation magnetization of metallic cobalt; B_C is the coercive field; B_T is the threshold value of the magnetic anisotropy field above which the magnetization becomes uniform over the entire volume of the sample; and N and $\langle V\rangle$, as in relationship (1), are the varied values of the concentration of cobalt nanoparticles and their average volume, respectively. The proposed expression (2) best describes the behavior of the ferromagnetic system (Fig. 3, solid curve *4*). The parameters of the simulation of the superparamagnetic and ferromagnetic samples of the nanocomposite materials under investigation, as well as the average diameters of cobalt nanoparticles, which were calculated from the volume under the assumption of their spherical shape, are listed in the table.

Therefore, the analysis of the results of magnetic investigations allows us to make the inference that the size of ion-synthesized cobalt nanoparticles in the amorphous silicon dioxide matrix is approximately equal to 4–5 nm and that the observed crossover from the superparamagnetic response to the ferromagnetic response of the nanocomposite system is associated with the increase in the nanoparticle number density in the implanted layer. It should be noted that the dispersion parameters obtained are in agreement with the electron microscopic observations of ion-synthesized cobalt nanoparticles in silica glass matrices [8–10].

Calculated values of the concentration, average volume, and average size of cobalt nanoparticles synthesized in the amorphous SiO_2 matrix at different implantation doses

Ion dose, 10^{17} ions/cm^2	Particle concentration, 10^{18} cm^{-3}	Average volume, nm^3	Average diameter, nm
0.50	3.4	37.8	4.2
0.75	5.1	44.6	4.4
1.00	5.9	61.6	4.9

3.2. Magneto-Optical Effects

The Faraday effect in the nanocomposite materials synthesized is determined by several contributions: the diamagnetic rotation of the SiO_2 matrix, the paramagnetic rotation of noninteracting cobalt ions, and the rotation of cobalt ions involved in clusters and/or nanoparticles. The contributions of cobalt were determined as the difference between the spectra measured for each of the samples implanted at the doses $D = 0.25 \times 10^{17}$, 0.50×10^{17}, 0.75×10^{17}, and 1.00×10^{17} ions/cm^2 and the spectrum of the SiO_2 matrix. These contributions are shown in Fig. 5 by curves *1–4*, respectively. It is evi-

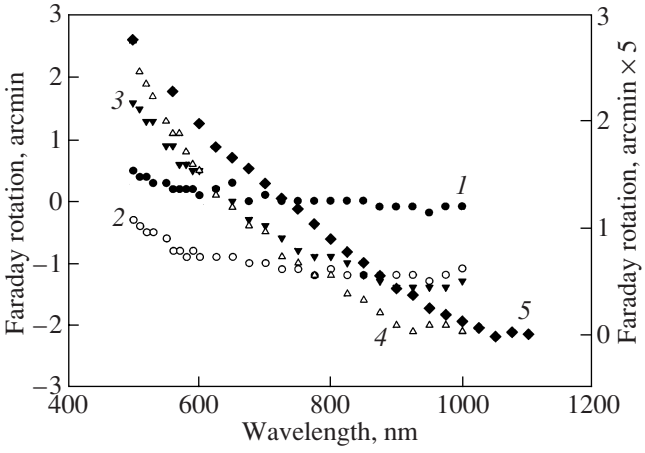

Fig. 5. Spectra of the Faraday rotation for (*1–4*) the samples implanted at different ion doses (minus the Faraday rotation in the matrix) and (*5*) the Co/SiO_2 multilayer film [15] (right scale). D = (*1*) 0.25, (*2*) 0.50, (*3*) 0.75, and (*4*) 1.00×10^{17} ions/cm^2. The magnetic field is 0.2 T. $T = 300$ K.

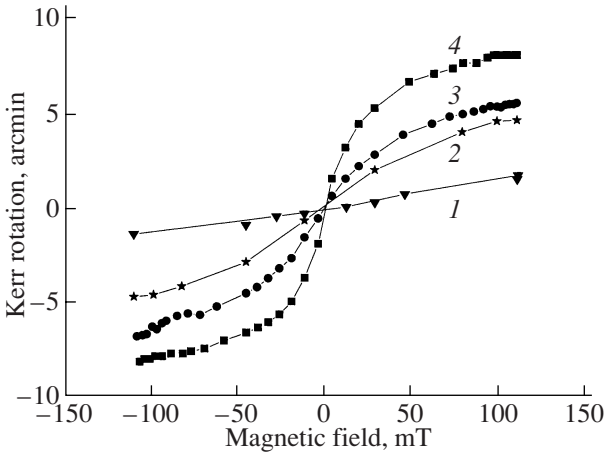

Fig. 6. Field dependences of the meridional Kerr effect for the samples implanted at the ion doses D = (*1*) 0.25, (*2*) 0.50, (*3*) 0.75, and (*4*) 1.00×10^{17} ions/cm^2. λ = 550 nm. T = 300 K.

dent that none of these curves can be described by the known formula for the paramagnetic rotation

$$\alpha_{para} = \frac{A\lambda}{(\lambda^2 - \lambda_0^2)}, \quad (3)$$

where A and λ_0 are a constant and the effective wavelength associated with the paramagnetic ions. Moreover, these curves do not correspond to the data available in the literature for uniform ferromagnetic cobalt layers. According to [14], the Faraday effect for a uniform ferromagnetic cobalt film in the visible range is positive and its magnitude increases with an increase in the wavelength λ and reaches a maximum in the vicinity of the wavelength $\lambda = 1.2$ μm (see [14, Fig. 14]). We can assume that the change in the spectral dependences of the Faraday effect with an increase in the implantation dose is governed by the increase in the amount of cobalt involved in ferromagnetic nanoparticles. At the minimum ion dose D, cobalt, as can be judged from the magnetic measurements, is predominantly incorporated into the matrix in the form of isolated paramagnetic ions. However, most likely, an insignificant number of Co ions are already joined together into nanoparticles with a magnetic ordering. The competition between the paramagnetic and ferromagnetic contributions of different signs to the Faraday effect leads to its very small magnitude (Fig. 5, curve *1*), whereas the contributions made to the magnetization curves by cobalt in any state have one sign and an insignificant amount of the ferromagnetic phase does not manifest itself. At higher doses, the ferromagnetic contribution is dominant; however, the shape of the spectra differs radically from the shape of the spectrum of the Faraday rotation obtained in [14]. The observed changes in the spectra of the Faraday rotation for the nanocomposite material as compared to the uniform cobalt film can be associated with the excitation and scattering of conduction electrons in the bounded volume of cobalt nanoparticles. The magneto-optical effects in similar media were theoretically investigated in the framework of the

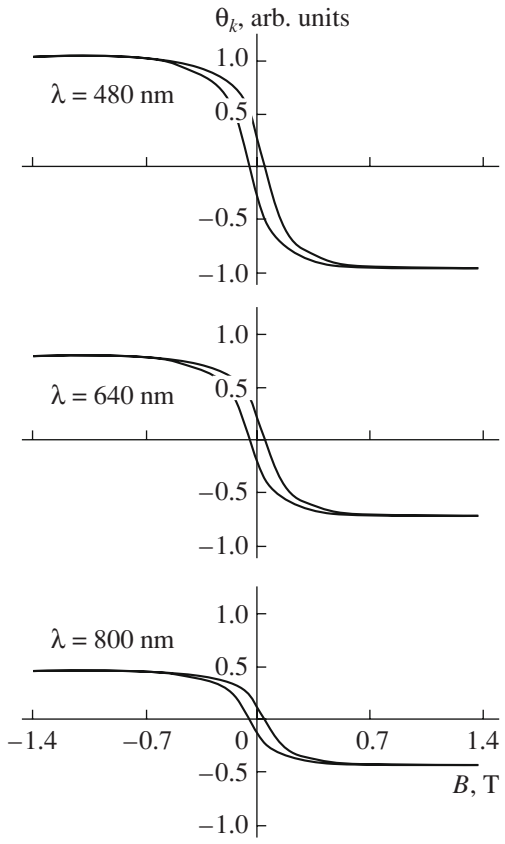

Fig. 7. Field dependences of the polar Kerr effect for the sample implanted at the ion dose $D = 0.75 \times 10^{17}$ ions/cm^2 for three wavelengths λ. Hysteresis loops are inverted with respect to the hysteresis loops obtained in magnetic measurements due to the negative sign of the polar Kerr effect.

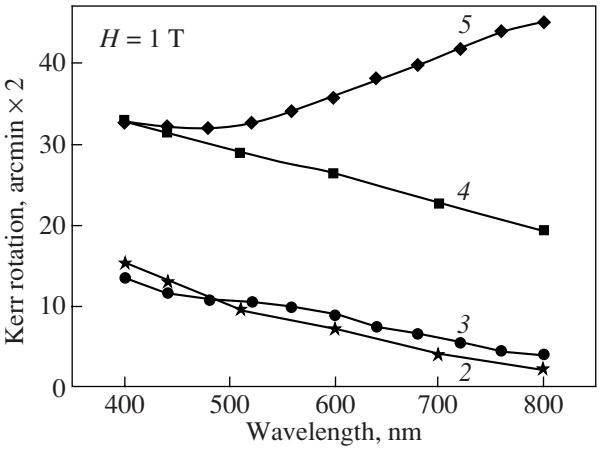

Fig. 8. Spectral dependences of the polar Kerr effect (magnitude) for the samples implanted at the ion doses D = (*2*) 0.50, (*3*) 0.75, and (*4*) 1.00×10^{17} ions/cm^2 and (*5*) the uniform cobalt film in a magnetic field of 1 T. T = 300 K.

effective-medium approximation in [3, 4] and experimentally observed in [4, 15]. It was revealed the spectra of the equatorial Kerr effect [4] and the Faraday rotation [15] substantially depend on the optical constants of the materials of the matrix and nanoparticles, their volume, and filling density. In particular, curve *5* in Fig. 5 corresponds to the spectrum of the Faraday rotation in the Co/SiO_2 granular film containing 20 pairs of Co and SiO_2 layers 2 and 10 nm thick, respectively [15]. The shape of the spectrum of the Faraday rotation for the film is similar to those for the samples implanted at the doses $(0.75–1.00) \times 10^{17}$ ions/cm^2; however, the rotation for the film remains positive over the entire spectral range, whereas the rotation for the samples under investigation changes sign in the vicinity of the wavelength $\lambda = 650$ nm. Therefore, the situation with implanted layers is more complex, possibly, also due to the nonuniform distribution of cobalt nanoparticles in the matrix (Fig. 1).

The field dependences of the meridional Kerr effect for all four samples are plotted in Fig. 6. It can be seen from this figure that these dependences are similar to the magnetization curves depicted in Fig. 3. (The absence of the hysteresis loop in the field dependence of the Kerr effect of the sample implanted at the maximum dose as compared to the magnetization curve for the same sample is most likely associated with the lower sensitivity of the setup for measuring the meridional Kerr effect.) Unlike the Faraday effect, the contribution to which can be made by cobalt ions in any state, the Kerr effects are due to the cobalt ions incorporated into the ferromagnetic particles or layers. Judging from the shape of the dependences of the Kerr effect and the ratio between the magnitudes of the effect in the maximum magnetic field for different samples, we can argue that the sample implanted at the minimum dose $D = 0.25 \times 10^{17}$ ions/cm^2 contains some amount of ferromagnetic cobalt. This agrees with the corresponding assumption made in the discussion of the Faraday effect. An increase in the implantation dose from $D = 0.25 \times 10^{17}$ ions/cm^2 to $D = 0.50 \times 10^{17}$ ions/cm^2 leads to a considerable increase (not proportional to the dose) in the amount of ferromagnetic cobalt. Most likely, in the vicinity of the above dose, there is a percolation threshold above which a layer with a high number density of cobalt nanoparticles is formed. This is evidenced by the field dependences of the polar Kerr effect (Fig. 7). At all doses in the range $D = (0.5–1.0) \times 10^{17}$ these dependences are represented by similar curves with a saturation and hysteresis, which are characteristic of thin layer with an in-plane anisotropy. The saturation field in the case of the polar magnetization is approximately equal to 0.6 T. Therefore, despite the amorphous state of the matrix, its layer implanted with cobalt exhibits an in-plane anisotropy. However, unlike the situation with cobalt nanoparticles in rutile single crystals [5] for which the field dependence of the magnetization exhibits a ferromagnetic behavior in the implanted plane and an antiferromagnetic behavior in the direction perpendicular to the implanted plane, in our case, the field dependence of the magnetization in both geometries is characterized by a ferromagnetic behavior. It should be noted that the hysteresis loops (even if very narrow) are also observed in the polar geometry. This circumstance can be one more argument confirming the fact that the layer with cobalt nanoparticles even at maximum implantation doses is not continuous.

As in the case of the Faraday effect, the spectra of the meridional and polar Kerr effects of the samples under investigation (Fig. 8) differ substantially from those of uniform cobalt films. The spectrum measured for the polar Kerr effect in the cobalt film on the same setup is represented by curve *5* in Fig. 8. The similarity between the spectra of the nanocomposite samples and their radical difference from curve *5* also indicate that the region with the highest number density of nanoparticles is not an analog of the continuous uniform film. It is clear that this region consists of nanoparticles with the filling density close to the percolation threshold. Therefore, the magnetic properties of this region are similar to those of continuous films, whereas the magneto-optical spectra are determined by the electronic processes in the closed volume of each particle.

4. CONCLUSIONS

Thus, the performed investigation of the field dependences of the magneto-optical effects for two orientations (parallel and perpendicular) of the external magnetic field with respect to the plane of the silica glass implanted with cobalt ions revealed that an increase in the implantation dose is accompanied by the transformation of the samples from the paramagnetic state into the superparamagnetic state and, finally, into the ferromagnetic state at room temperature. By using the results of magnetic measurements, the average size of cobalt nanoparticles formed upon implantation was estimated to be ~4–5 nm. It was demonstrated that an increase in the implantation dose results in an increase in the density of filling of the implanted layer by nanoparticles.

It was revealed that the spectral dependences of the Kerr and Faraday effects for the samples under investigation differ radically from those for homogeneous cobalt samples. For example, the magnitude of both effects for the homogeneous samples in the spectral range under investigation increases with an increase in the light wavelength, whereas for the implanted samples, the magnitude of the Kerr effect by contrast increases with a decrease in the wavelength and the Faraday effect changes sign in the vicinity of the wavelength $\lambda = 600$ nm. Hypothetically, these differences are associated with the excitation and scattering of conduction electrons in the bounded volume of cobalt nanoparticles.

Therefore, in the present work, it was shown that the ion beam implantation technique can be used with advantage to synthesize cobalt nanoparticles in dielectric matrices in order to fabricate composite materials that exhibit magneto-optical effects and can be practically applied in various devices for recording and storage of information.

ACKNOWLEDGMENTS

We would like to thank the Alexander von Humboldt Foundation (Germany) for the financial support of A.L. Stepanov in Germany.

This study was supported by the Russian Foundation for Basic Research (project nos. 04-02-97505-r_ofi, 06-02-08147_ofi, 07-02-92174-CNRS) and the Branch of General Physics and Astronomy of the Russian Academy of Sciences (Program "New Materials and Structures"). R.D. Ivantsov acknowledges the support of the Russian Science Support Foundation.

REFERENCES

1. N. A. Tolstoĭ and A. A. Spartakov, *Electro-Optics and Magneto-Optics of Dispersed Systems* (St. Petersburg State University, St. Petersburg, 1996) [in Russian].
2. A. K. Zvezdin and V. V. Kotov, *Modern Magneto-Optics and Magneto-Optical Materials* (Institute of Physics, London, 1997).
3. T. K. Xia, P. M. Hui, and D. Stroud, J. Appl. Phys. **67**, 2736 (1990).
4. E. A. Gan'shina, M. V. Vashuk, A. N. Vinogradov, A. B. Granovsky, V. S. Gushchin, P. N. Shcherbak, Yu. E. Kalinin, A. V. Sitnikov, Chong-Oh Kim, and Cheol Gi Kim, Zh. Éksp. Teor. Fiz. **125** (5), 1172 (2004) [JETP **98** (5), 1027 (2004)].
5. R. I. Khaibullin, L. R. Tagirov, B. Z. Rameev, Sh. Z. Ibragimov, F. Yildiz, and B. Aktas, J. Phys.: Condens. Matter **16**, L443 (2004).
6. A. L. Stepanov and I. B. Khaibullin, Rev. Adv. Mater. Sci. **9**, 109 (2005).
7. A. L. Stepanov, V. A. Zhikharev, and I. B. Khaĭbullin, Fiz. Tverd. Tela (St. Petersburg) **43** (4), 733 (2001) [Phys. Solid State **43** (4), 766 (2001)].
8. O. Cintora-Gonzalez, D. Muller, C. Estournes, M. Richard-Plouet, R. Poinsot, J. J. Grob, and J. Guille, Nucl. Instrum. Methods Phys. Res., Sect. B **178**, 144 (2001).
9. E. Cattaruzza, F. Gonella, G. Mattei, P. Mazzoldi, D. Gatteschi, C. Sangregorio, M. Falconieri, and G. Salvetti, Appl. Phys. Lett. **73**, 1176 (1998).
10. M. Klimenkov, J. von Boraby, W. Matz, D. Eckert, M. Wolf, and K.-H. Müller, Appl. Phys. A: Mater. Sci. Process. **74**, 571 (2002).
11. P. D. Townsend, P. J. Chandler, and L. Zhang, *Optical Effects of Ion Implantation* (Cambridge University Press, Cambridge, 1994).
12. M. E. McHenry, S. A. Majetich, J. O. Artamn, M. DeGraef, and S. W. Stale, Phys. Rev. B: Condens. Matter **49**, 11358 (1994).
13. A. L. Geiler, V. G. Harris, C. Vittoria, and N. X. Sun, J. Appl. Phys. **99**, 08B316 (2006).
14. H. Clemens and J. J. Jaumann, Z. Phys. **173**, 135 (1963).
15. Y. A. Dynnik, I. S. Edelman, T. P. Morozova, P. D. Kim, I. A. Turpanov, and A. Y. Betenkova, Opt. Mem. Neural Network **17**, 274 (1998).

Translated by O. Borovik-Romanova